Electrochemical Lithium Insertion for Perovskite Oxides of $Li_yLa_{(1-y)/3}NbO_3$ ($y = 0, 0.1, 0.25$)

Masanobu Nakayama, Kazuomi Imaki, Hiromasa Ikuta, Yoshiharu Uchimoto, and Masataka Wakihara*

Department of Applied Chemistry, Graduate School of Science and Engineering, Tokyo Institute of Technology, Ookayama, Meguro-ku, Tokyo 152-8552, Japan

Received: March 31, 2002; In Final Form: May 8, 2002

The relationship between crystal structure and electrochemical behavior through the lithium insertion in the perovskite oxides, $Li_yLa_{(1-y)/3}NbO_3$ ($y = 0$, 0.1, 0.25), has been investigated. The results of the relationship between the amount of inserted lithium and the number of vacancies reveal that Li^+ ions insert into the vacancies at an A-site. Furthermore, observed cell potential diagrams indicate that the Li^+ insertion reaction occurs stepwise, since there are two kinds of vacancy sites due to the ordering arrangement of cations in the A-site. With increasing the composition *y*, the extinction of electrochemical behavior due to such stepwise reaction was observed, which is attributed to the disordering of cation arrangement. Simple Coulombic calculation of electrochemical lithium insertion also supports the observed electrochemical behavior and determines the insertion step to the two kinds of vacancy sites.

1. Introduction

An increasing interest developed around transition-metal oxides with lithium insertion sites as the cathode material of high energy density lithium ion batteries.[1] These materials are attractive not only for commercial use but also as model materials for the basic study of solid-state electrochemical reactions. This is why such model materials are suitable for theoretical treatment, such as ab initio calculation,[2−6] lattice gas model simulation,[7] and so on,[8,9] since the host crystal structure is almost same between before and after electrochemical reaction.

A-site deficient perovskite type oxides, $La_{1/3}NbO_3$, are considered to be a candidate of these model compounds, because this compound has relatively simple structure. The crystal structure of pristine material, $La_{1/3}NbO_3$, was first described by Iymer and Smith.[10] As shown in Figure 1, La ions and vacancies at A-sites are ordered within alternate (001) planes, doubling the *c*-parameter of the cubic perovskite-type cell and leading to a slightly distorted orthorhombic lattice with parameters $a \sim a_p$, $b \sim b_p$, $c \sim 2a_p$ (p refers to the cubic-perovskite unit cell). Hereinafter we express the vacancies at the La rich layer and the completely empty layer as V_{La} and V_{vac}, respectively (see Figure 1). According to Belous et al.,[11] the crystal symmetry changed from orthorhombic to tetragonal and then to cubic with increasing the composition *y* in $Li_yLa_{(1-y)/3}NbO_3$. In our previous study,[12] powder XRD patterns of the samples $y \leq 0.05$ were indexed in an orthorhombic system. In the composition $y \geq 0.1$ the crystal structure changes to the tetragonal system, and then all the lattice parameters *a*, *b*, and *c* become equal at the composition $y = 0.25$. The peak intensity of superlattice $(0\ 0\ 1/2)_p$ due to cation and vacancy ordering in A-sites decreases with increasing the composition *y*. Therefore it was expected that ordering of A-site cations are destroyed and randomly distributed at the A-site. Recently through the electron diffraction study,[13] the decreasing of ordered arrangement of cations seems to be explained by the existence of a microdomain structure with three different orientations of the *c*-axis in the samples.

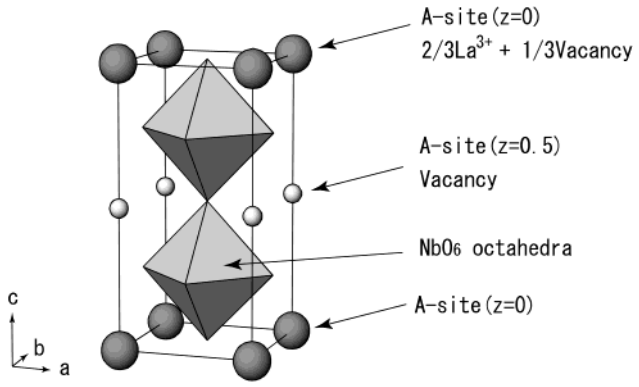

Figure 1. Crystal structure of $La_{1/3}NbO_3$.

The electrochemical insertion of lithium expresses as follows:

$$x\mathrm{Li} + \mathrm{Li}_y\mathrm{La}_{(1-y)/3}\mathrm{NbO}_3 \rightarrow \mathrm{Li}_x\mathrm{Li}_y\mathrm{La}_{(1-y)/3}\mathrm{NbO}_3 \qquad (1)$$

hereinafter *x* means the molar composition of electrochemically inserted lithium ions, and *y* means the molar amount of substitution $3Li^+$ for La^{3+}, or thermally inserted lithium ions in this paper. The electrochemical insertion of lithium in pristine material, $La_{1/3}NbO_3$, has been reported by Nadiri et al.,[14] and they confirmed that the host structure of $La_{1/3}NbO_3$ kept during the insertion reaction using X-ray diffraction measurement. From the cell potential diagram, they suggested that lithium ions first insert to the V_{vac} vacancy and then insert to V_{La} vacancies. Furthermore, in the solid-solution $Li_yLa_{(1-y)/3}NbO_3$, the cyclic voltammetry measurement has been already investigated.[15] However, the scanning rate is relatively high in the experiment[15] because authors aimed to investigate the electrochemical window of the material as a solid electrolyte. Therefore, the exact redox potential of these solid-solution is still uncertain.

* Corresponding author. Telephone: + 81 3 5734 2145. Fax: +81 3 5734 2146. E-mail: mwakihar@o.cc.titech.ac.jp.

10.1021/jp0258659 CCC: $22.00 © 2002 American Chemical Society
Published on Web 05/25/2002

In this paper we investigate electrochemical behavior of lithium insertion for the solid solution $Li_yLa_{(1-y)/3}NbO_3$ and discuss the relationship with crystal structure mentioned above.

2. Experimental Section

Different compositions of the $Li_yLa_{(1-y)/3}NbO_3$ ($y = 0$, 0.1, 0.25) solid solution were prepared by conventional solid-state reaction, as described in ref 12, from stoichiometric amounts of Li_2CO_3 (99.9%), La_2O_3 (99.9%), and Nb_2O_5 (99.9%), (Soekawa Chemical Industries, Limited). The mixture of reagents was heated at 800 °C for 2 h and then at 1200 °C for 24 h in air with several intermittent grindings. In case of $La_{1/3}NbO_3$ ($y = 0$), the synthesized temperature was at 1300 °C to obtain single phase samples. Crystalline phase identification and the evaluation of lattice parameters were carried out by powder X-ray diffraction using a Rigaku RINT2500V diffractometer with Cu Kα radiation, a curved graphite monochromator, and the results were consistent with our previously reported data.[12]

Electrochemical measurements for Li insertion were carried out using a three-electrode cell. Li foil (Aldrich) was used as counter and reference electrodes, and a 1 M solution of $LiClO_4$ in anhydrous ethylene carbonate (EC) and diethylene carbonate (DEC) was used as electrolyte (Tomiyama Pure Chemical Company, Limited). The working electrode was the mixture of 90 wt % perovskite powders, 7 wt % acetylene black as a current collector, and 3 wt % poly(tetrafluoroethylene) (PTFE) binder. Li foils and the mixture of working electrode was pressed onto Ni-mesh. Electrochemical lithium insertion was carried out by an interrupted galvanostatic method and slow speed liner potential sweep method (0.05 mV/s) using a Solartron 1287 electrochemical interface. The interrupted galvanostatic measurement is performed by repeats of the flowing galvanostatic current (current density; 40 μA/cm^2) at $x = 0.02$ interval and then monitoring the potential relaxation (up to 12 h) under open circuit state. The preparation of the cells and electrochemical experiments were performed in an argon-filled glovebox.

3. Results

Figure 2 shows the potential diagram for lithium insertion of the pristine material $La_{1/3}NbO_3$ by the interrupted galvanostatic method at $x = 0.02$ intervals. The time dependent relaxation behavior is also shown in Figure 3 at the composition $x = 0.2$, 0.4, 0.6, 0.8. From Figure 3, samples with lower amounts of x relaxed in several hours; however, samples with $x > 0.7$ were not completely relaxed to equilibrium state after 30 h. These results indicate that relaxation time of the lithium diffusion to achieve the homogeneous lithium distribution in the solid at lower amount of x is much shorter than that at $x > 0.7$, and the reaction process is completely different from each other for the samples with $x < 0.7$ and $x > 0.7$. In addition, the potentials decreased from 1.2 V plateau to less than 1.0 V under flowing current condition. This indicates that lithium insertion into acetylene black occurred as shown in Figure 2. Therefore it is hard to estimate accurately the relationship between equilibrium potential and composition, and we do not discuss further the electrochemical behavior at the region of cell potential < 1.0 V in this paper.

The equilibrium potential (each peak top of the cell potential diagram shown in Figure 2) of $Li_xLa_{1/3}NbO_3$ ($x < \sim 0.7$) was almost consistent with previously reported data.[14] The equilibrium potential monotonically decreased in the composition range

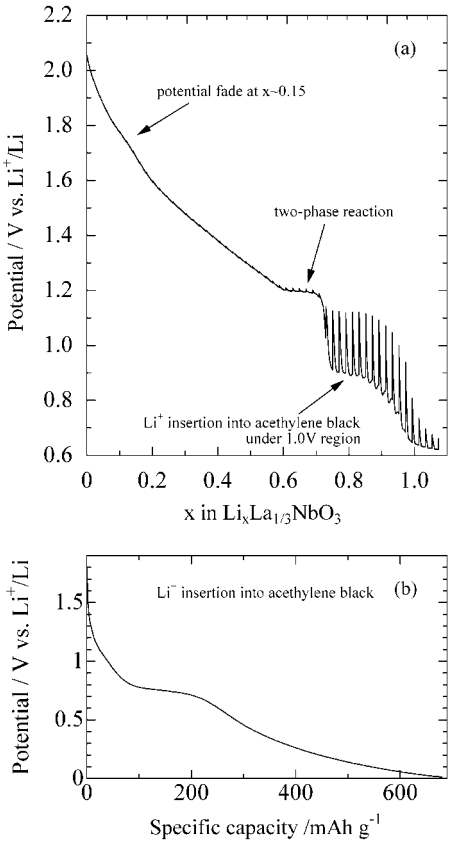

Figure 2. (a) Variation of the potential with Li^+ insertion by the interrupted galvanostatic method for $Li_xLa_{1/3}NbO_3$. (b) Variation of the potential with Li^+ insertion into acetylene black as a reference.

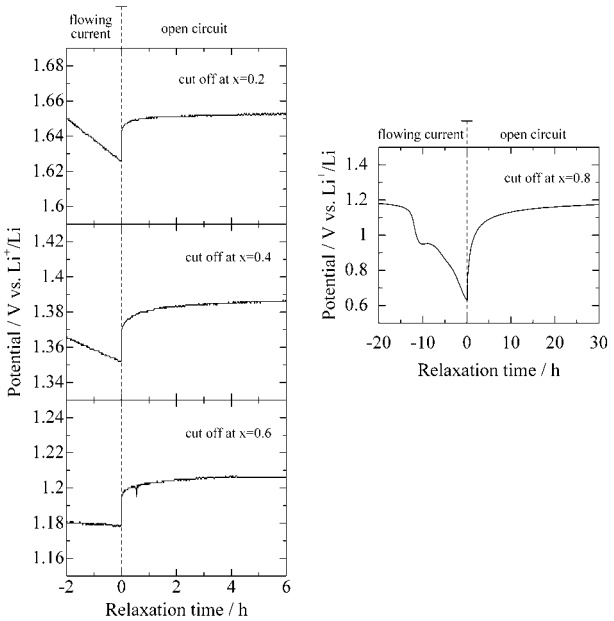

Figure 3. Time-dependent potential behavior for $Li_xLa_{1/3}NbO_3$ ($x =$ 0.2, 0.4, 0.6, 0.8).

from $x = 0$ to $x \sim 0.58$, indicating the solid-solution reaction;[8] however, from $x \sim 0.58$ to $x \sim 0.66$ the potential remained unchanged, indicating the two-phase reaction.[8] In addition, the equilibrium cell potential was slightly faded at the composition of $x \sim 0.15$, and this behavior has not been mentioned previously to the author's knowledge. The diagram of slow speed liner potential sweep measurement was shown in Figure 4. There are two cathodic peaks in the range from 2.7 to 1.0 V. One of

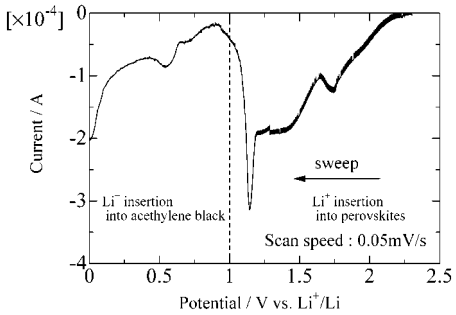

Figure 4. Slow speed liner potential sweep measurement for $Li_xLa_{1/3}NbO_3$.

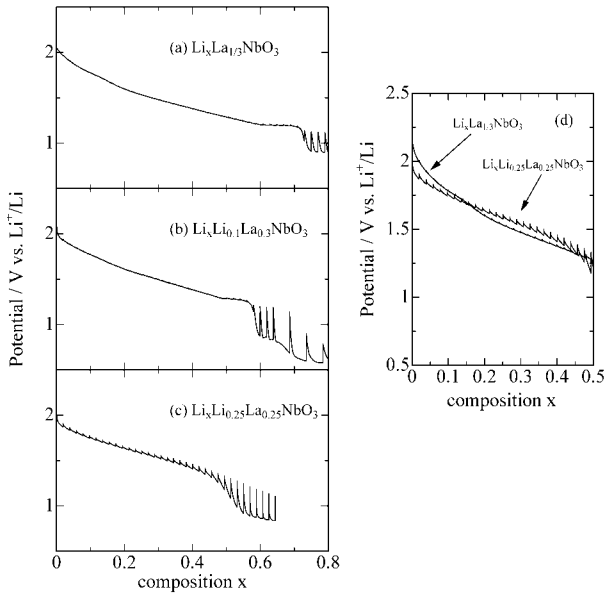

Figure 5. Variation of the cell potential with Li^+ insertion by the interrupted galvanostatic method for (a) $Li_xLa_{1/3}NbO_3$, (b) $Li_xLi_{0.1}La_{0.3}NbO_3$, and (c) $Li_xLi_{0.25}La_{0.25}NbO_3$, and (d) comparison the cell potential between $Li_xLa_{1/3}NbO_3$ and $Li_xLi_{0.25}La_{0.25}NbO_3$.

the peaks at higher potential (~1.75 V) correlated to potential fade at $x \sim 0.15$, and the other at lower potential (~1.1 V) correlated to the two-phase reaction from $x \sim 0.58$ to $x \sim 0.66$.

Figure 5 shows the comparison of cell potential diagrams of the samples with several composition y in $Li_yLa_{(1-y)/3}NbO_3$. The potential drop from ~1.2 V to <1.0 V occurred at the composition $x \sim 0.66$, ~ 0.58, ~ 0.50 for the samples with $y = 0$, 0.1, 0.25, respectively. In the initial part ($0 \le x \le 0.15$) of the insertion the equilibrium potential slightly decreases with increasing the composition y, while that of the following part ($x > 0.15$) increases with y (Figure 5d). This indicates that the equilibrium potential was averaged over the whole the range of the composition x, when the composition y increases. In addition, both of the potentials fade at the composition of $x \sim 0.15$, and the potential plateau of the two-phase reaction from $x \sim 0.58$ to 0.66, observed in the samples of $y = 0$, disappeared with increasing the composition y. This behavior was clearly seen from the results of slow speed linear potential sweep measurements shown in Figure 6. The cathodic peak of ~1.75 V corresponding to the potential fade and the current peak of ~1.2 V corresponding to the two-phase reaction were decreasing from $y = 0$ to $y = 0.1$ and completely disappeared at $y = 0.25$.

4. Discussion

In this section, we discuss the results of electrochemical behavior with regard to the crystal structure mentioned in the introduction section. Especially we focused on the lithium distribution in the perovskite compounds. Because it is difficult to determine the insertion site of lithium ion by conventional X-ray diffraction techniques due to low X-ray scattering ability of lithium, we attempt to discuss the distribution of inserted lithium ions in perovskite compounds by analyzing the relationship between the cell potential behavior and the amount of inserted lithium ions.

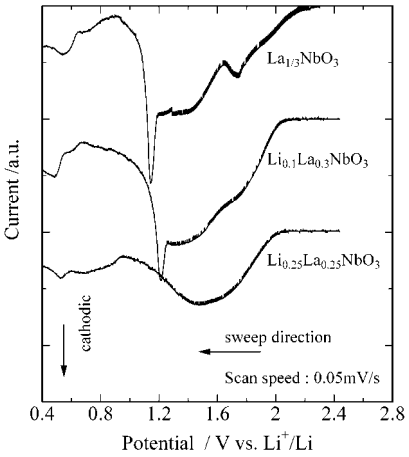

Figure 6. Comparison of the slow-speed linear potential sweep measurement for $Li_xLi_yLa_{(1-y)/3}NbO_3$ ($y = 0$, 0.1, 0.25).

As shown in Figure 2, the total amount of inserted lithium ions up to 1.0 V (before the insertion of lithium into acetylene black occurred) decreases with increasing the composition y. The total amount of inserted lithium is $x \sim 0.70$, ~0.58, and ~0.50, for $y = 0$, 0.1, and 0.25, respectively. There are two kinds of vacant A-sites in $La_{1/3}NbO_3$, V_{La} and V_{vac}, respectively (see Figure 1), and the total number of vacancies V_{La} and V_{vac} corresponds to the composition $x = 0.667$, 0.6, and 0.5 for the perovskites with $y = 0.0$, 0.1, and 0.25, respectively. From the consistency between the amount of inserted lithium ions and vacancy sites, it is concluded that lithium ions are electrochemically inserted into V_{La} and V_{vac} vacancies. Similar behavior is also observed in $La_{0.50}Li_{0.37}TiO_{2.94}$ perovskite compounds.[16] To determine how lithium ions insert to the two kinds of vacancy sites in perovskite V_{La} and V_{vac}, the variation of Coulombic energy (which is a main part of lattice stabilized energy) with lithium ion insertion was calculated under constant volume condition. Coulombic energy was calculated from following equations:

$$U_i = \sum_j \frac{Z_j e}{4\pi\epsilon_0 r_{ij}} \tag{2a}$$

$$U_{\text{Coulomb}} = N_i Z_i U_i \tag{2b}$$

where U_i and U_{Coulomb} indicate the site potential of the site i and total Coulombic energy per unit cell, respectively. Ze means electrical charge of ions, ϵ_0 is dielectric constant in a vacuum, and r_{ij} is interionic distance between ions i and j. N_i is the number of ions i in the unit cell. Table 1 shows the parameters using this calculation based on crystal structure information and ion and charge distribution. Initial ion arrangement was based on ref 10, the lattice parameters were determined as cubic root of the cell volume, and fractional coordinates of each ion were referred as ideal cubic perovskites. It was assumed that the reaction occurred under constant volume conditions. The validity of Coulombic calculation under constant volume conditions is based on the fact that volume change through the lithium

TABLE 1: Parameters[a] of Modeled Crystal Structure and Charge Distribution for Calculation of Coulombic Energy

site	ion	occupancy	average charge	fractional coordinates
1*a* (A_{La})	La^{3+}	2/3	$2/3 \times 3$	(0, 0, 0)
	Li^+	$g_{Li}(V_{La})$	$g_{Li}(V_{La})$	
1*b* (A_{vac})	Li^+	$g_{Li}(V_{vac})$	$g_{Li}(V_{vac})$	(0, 0, 1/2)
2*h*	Nb^{5+}	1	$5 - [g_{Li}(V_{vac}) + g_{Li}(V_{La})]/2$	(1/2, 1/2, 1/4)
4*i*	O^{2-}	1	-2	(1/2, 0, 1/4)
1*c*	O^{2-}	1	-2	(1/2, 1/2, 0)
1*d*	O^{2-}	1	-2	(1/2, 1/2, 1/2)

[a] $Li_xLa_{1/3}NbO_3$; space group: *P4/mmm* (No. 123); lattice parameter: $a = b = 3.98$ Å, $c = 7.89$ Å, $\alpha = \beta = \gamma = 90°$.

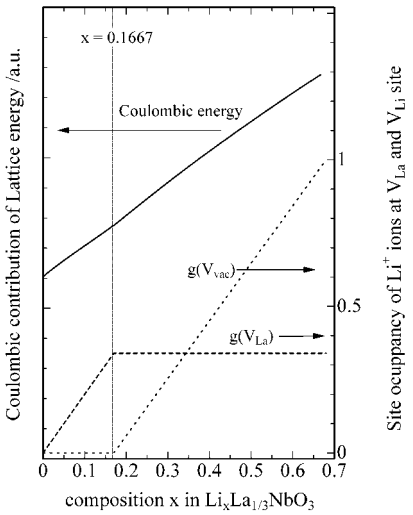

Figure 7. Variation of Coulombic energy and site occupancy of Li^+ with lithium insertion under energetically optimum conditions.

insertion reaction is quite small (the cell volume increases only 0.3% from $x = 0$ to 0.8, from ref 14). The values of $g_{Li}(V_{La})$ and $g_{Li}(V_{vac})$ in Table 1 indicate site occupancy of lithium ions in each vacancy sites, V_{La} and V_{vac}, respectively. The relationship of $g_{Li}(V_{La})$, $g_{Li}(V_{vac})$, and composition x were expressed as following equation:

$$x = 1/2\,[g_{Li}(V_{La}) + g_{Li}(V_{vac})] \tag{3}$$

The charges of La, Li, and O ions were assigned conventional values of +3, +1 and −2, respectively, based on the octet rule. To maintain charge neutrality, the valence state of Nb ions should be changed as reductive species from +5 to +4 with lithium insertion. The Coulombic energy calculation consists of the cycles of following steps from $x = 0$ to $x = 2/3$: (1) add the value +0.01 for the $g_{Li}(V_{La})$ and calculate the Coulombic energy U_1 (this step is skipped in case of $g_{Li}(V_{La}) > 1/3$); (2) add the value +0.01 for the $g_{Li}(V_{vac})$ and calculate the Coulombic energy U_2 (this step is skipped in case of $g_{Li}(V_{vac}) > 1$); and (3) Revise the parameter shown in Table 1 with lower Coulombic energy $U_{Coulomb}$

The results of the calculation shown in Figure 7 indicate that the lithium ions initially insert into the V_{La} site until it is fully occupied and then insert into V_{vac} site. The slope of Coulombic energy is slightly changed at the composition $x = 0.167$. These calculation results are consistent with the experimental data, the cell potential fade at $x \sim 0.15$ shown in Figure 2. Therefore it is concluded that the occupation of lithium ions in vacancy sites V_{La} is preferable to V_{vac} energetically, and the insertion reactions are carried out stepwise.

Next we discuss the electrochemical behavior depending on the composition y in $Li_xLi_yLa_{(1-y)/3}NbO_3$. As mentioned in the results section, the potential fade at $x \sim 0.15$ and cathodic current peak at ~1.75 V, which corresponds to the stepwise reaction of lithium insertion, are disappearing with increasing the composition y. In addition, the cell potential in the whole range of composition x was averaged by increasing the composition y. The observed electrochemical behavior could be explained in view of the crystal structure. A-site cations are disordering with increasing the substitution amount of Li^+ for La^{3+} ions,[11,12] and this disordering could unify the difference of the site potential for the vacancies V_{La} and V_{vac}. Therefore, the extinction of stepwise lithium insertion at $x \sim 0.15$ may be due to the unification of the site potential in the two of vacancy sites. The averaged cell potential at larger y composition also results from the extinction of the difference of the site potential due to the disordered cation arrangement.

In the samples with lower composition y, the potential plateau due to the two-phase reaction is observed at the end part of lithium insertion. This plateau also disappeared with increasing the composition y. Therefore, this two-phase reaction may relate to the cation distribution in the A-site. Similar behavior has been reported on the spinel oxides, $LiMn_2O_4$,[17] and it has been suggested that the potential plateau is due to the ordering phase of lithium ions from the simulation such as lattice-gas model.[7] In this study, ordering arrangement of lithium ions might occur at the potential plateau for the sake of minimizing the Coulombic repulsion, and the extinction of potential plateau at higher y composition is considered to be the result from random distribution of lanthanum ions in the A-site which interrupts the ordering arrangement.

5. Conclusion

Electrochemical insertion to A-site deficient perovskite oxides, $Li_xLi_yLa_{(1-y)/3}NbO_3$ ($y = 0$, 0.1, 0.25) has been carried out. Lithium ions are inserted into the vacancies at A-sites consistent with the amount of inserted Li^+ ions and the number of vacancies in the A-site. In the sample with composition $y = 0$, there are two kinds of vacancy sites, V_{La} and V_{vac}. V_{La} sites are energetically preferable for the lithium insertion and cause the stepwise lithium insertion. This is confirmed both by the results of electrochemical experiment (Figure 2 and Figure 4) and simple Coulombic calculation. A-site cations tends to become disordered in arrangement at higher composition y, and this disordering unifies the difference of site potential of two vacancy sites. Accordingly, it is concluded that stepwise lithium insertion disappeared due to disordered arrangement of A-site cations. In addition, distribution of A-site cations might also affect the two-phase reaction at the end part of lithium insertion.

Acknowledgment. This work was supported by Grant-in-Aid for Scientific Research on Priority Areas (B) (No. 740) "Fundamental Studies for Fabrication of All Solid State Ionic Devices" from Ministry of Education, Culture, Sports, Science and Technology. One of the authors, M.N., thanks the New Energy and Industrial Technology Development Organization for financial support of this work.

References and Notes

(1) In *Lithium Ion Batteries*; Wakihara, M., Yamamoto, O., Eds.; Kodansha: Tokyo, 1998.

(2) Zheng, T.; Dahn, J. R. *Phys. Rev. B* **1997**, *56*, 3800.

(3) Aydinol, M. K.; Kohan, A. F.; Ceder, G.; Cho, K.; Joannopoulos, J. *Phys. Rev. B* **1997**, *56*, 1354.

(4) Koyama, Y.; Kim, Y.-S.; Tanaka, I.; Adachi, H. *Jpn. J. Appl. Phys.* **1999**, *38*, 2024.
(5) Hibino, M.; Han, W.; Kubo, T. *Solid State Ionics* **2000**, *135*, 61.
(6) Liu, Y.; Fujiwara, T.; Yukawa, H.; Morinaga, M. *Electrochim. Acta* **2001**, *46*, 1151.
(7) Gao, Y.; Reimers, J. N.; Dahn, J. R. *Phys. Rev. B* **1996**, *54*, 3878.
(8) Goodenough, J. B.; Manthiram, A.; Wnetrzewski, B. *J. Power Sources* **1993**, *43*−*44*, 269.
(9) Yamaki, J.; Egashira, M.; Okada, S. *J. Power Sources* **2001**, *97*−*98*, 349.
(10) Iyer, P. N.; Smith, A. J. *Acta Crystallogr.* **1967**, *23*, 740.
(11) Belous, A. G.; Novitskaya, G. N.; Polyanetskaya, S. V.; Gornikov, Yu I. *Izv. Akad. Nauk SSSR, Neorg. Mater.* **1987**, 470.
(12) Kawakami, Y.; Ikuta, H.; Wakihara, M. *J. Solid State Electrochem.* **1998**, *2*, 206.
(13) García-Martín, S.; Alario-Franco, M. Á. *J. Solid State Chem.* **1999**, *148*, 93.
(14) Nadiri, A.; Le Flem, G.; Delmas, C. *J. Solid State Chem.* **1988**, *73*, 338.
(15) García-Martín, S.; Rojo, J. M.; Tsukamoto, H.; Morán, E.; Alario-Franco, M. Á. *Solid State Ionics* **1999**, *116*, 11.
(16) Shan, Y. J.; Chen, L.; Inaguma, Y.; Itoh, M.; Nakamura, T. *J. Power Sources*, **1995**, *54*, 397.
(17) Ohzuku, T.; Kitagawa, M.; Hirai, T. *J. Electrochem. Soc.* **1990**, *137*, 3769.